ErbB3 downregulation enhances luminal breast tumor response to antiestrogens

Meghan M. Morrison,[1] Katherine Hutchinson,[1] Michelle M. Williams,[1] Jamie C. Stanford,[1] Justin M. Balko,[2] Christian Young,[2] Maria G. Kuba,[2] Violeta Sánchez,[2] Andrew J. Williams,[1] Donna J. Hicks,[1] Carlos L. Arteaga,[1,2,3] Aleix Prat,[4,5,6] Charles M. Perou,[4,5,6] H. Shelton Earp,[4,7,8] Suleiman Massarweh,[9] and Rebecca S. Cook[1,3]

[1]Department of Cancer Biology and [2]Department of Medicine, Vanderbilt University School of Medicine, Nashville, Tennessee, USA. [3]Vanderbilt-Ingram Cancer Center, Nashville, Tennessee, USA. [4]Lineberger Comprehensive Cancer Center, [5]Department of Genetics, [6]Department of Pathology and Laboratory Medicine, [7]Department of Pharmacology, and [8]Department of Medicine, University of North Carolina, Chapel Hill, North Carolina, USA. [9]Department of Internal Medicine, University of Kentucky and Markey Cancer Center, Lexington, Kentucky, USA.

Aberrant regulation of the erythroblastosis oncogene B (ErbB) family of receptor tyrosine kinases (RTKs) and their ligands is common in human cancers. ErbB3 is required in luminal mammary epithelial cells (MECs) for growth and survival. Since breast cancer phenotypes may reflect biological traits of the MECs from which they originate, we tested the hypothesis that ErbB3 drives luminal breast cancer growth. We found higher *ERBB3* expression and more frequent *ERBB3* gene copy gains in luminal A/B breast cancers compared with other breast cancer subtypes. In cell culture, ErbB3 increased growth of luminal breast cancer cells. Targeted depletion of ErbB3 with an anti-ErbB3 antibody decreased 3D colony growth, increased apoptosis, and decreased tumor growth in vivo. Treatment of clinical breast tumors with the antiendocrine drug fulvestrant resulted in increased ErbB3 expression and PI3K/mTOR signaling. Depletion of ErbB3 in fulvestrant-treated tumor cells reduced PI3K/mTOR signaling, thus decreasing tumor cell survival and tumor growth. Fulvestrant treatment increased phosphorylation of all ErbB family RTKs; however, phospho-RTK upregulation was not seen in tumors treated with both fulvestrant and anti-ErbB3. These data indicate that upregulation of ErbB3 in luminal breast cancer cells promotes growth, survival, and resistance to fulvestrant, thus suggesting ErbB3 as a target for breast cancer treatment.

Introduction

Aberrant regulation of the erythroblastosis oncogene B (ErbB) family of receptor tyrosine kinases (RTKs) and their ligands is common in human cancers (1–4). This family consists of 4 related members, HER1/ErbB1/EGFR, HER2/ErbB2/Neu, HER3/ErbB3, and HER4/ErbB4. Except for ErbB3, which has very weak kinase activity, the ErbB RTKs exhibit dimerization-induced tyrosine phosphorylation and catalytic activation that results in signal transduction to intracellular targets. ErbBs are able to form homodimers as well as heterodimers with other coreceptors of the ErbB family. ErbB3 relies on transphosphorylation by heterodimeric partners to induce signal transduction (5–7). Therefore, therapeutic interest in the ErbB family has been historically focused on EGFR and ErbB2.

HER2/ErbB2 is gene amplified in nearly 25% of all breast cancers. Targeting HER2/ErbB2 activity using the monoclonal antibody trastuzumab or the small molecule tyrosine kinase inhibitor (TKI) lapatinib decreases growth of *HER2*-amplified breast cancer cells, improving survival and outcome of patients with breast cancers. Recently, clinical results demonstrate that therapeutic resistance to HER2/ErbB2 inhibitors occurs in part due to feedback upregulation of ErbB3 signaling, increasing the activity and output through the PI3K/mTOR pathway. This observation may underlie the recently published clinical success of the monoclonal antibody pertuzumab, which targets HER2/ErbB2 and prevents its heterodimerization with ErbB3 (8). It was recently demonstrated in genetically engineered mouse models that ErbB3 is required not only for maintaining the malignant phenotype of HER2/ErbB2-overexpressing mammary tumors (9), but also for the genesis of mammary tumors that overexpress HER2/ErbB2 and for premalignant changes to the mouse mammary epithelium caused by HER2/ErbB2 overexpression (10), consistent with the idea that HER2/ErbB3 heterodimers drive mitogenic signaling in the mammary epithelium.

However, expression analyses suggest that transgenic mouse models of HER2/ErbB2 overexpression in the mammary epithelium do not generate tumors resembling human *HER2*-enriched breast cancers. Instead, these tumors more closely resemble the luminal B subtype of human breast tumors (11), those that express estrogen receptor (ER) but are often not responsive to endocrine therapy. Because loss of ErbB3 prevented tumorigenesis in these mouse models of HER2/ErbB2 overexpression, it is possible that ErbB3 may play a wider role in the pathology of luminal B–like tumors that express HER2/ErbB2, but that are not necessarily gene amplified. This idea is supported by previous demonstrations that ErbB3 was required in the untransformed mouse mammary epithelium for growth and survival of progenitor and mature luminal cells of the ducts (12), but was not required for growth and survival of other epithelial populations in the mouse mammary gland (13, 14). Because many traits of a given breast cancer might reflect the untransformed breast epithelial cell from which the tumor originated (15, 16), these observations prompted us to test the hypothesis that ErbB3 drives growth and survival of luminal breast cancer cells in a manner that parallels its role in maintaining the untransformed luminal epithelium. We found

Conflict of interest: The authors have declared that no conflict of interest exists.

Note regarding evaluation of this manuscript: Manuscripts authored by scientists associated with Duke University, The University of North Carolina at Chapel Hill, Duke-NUS, and the Sanford-Burnham Medical Research Institute are handled not by members of the editorial board but rather by the science editors, who consult with selected external editors and reviewers.

Citation for this article: *J Clin Invest.* 2013;123(10):4329–4343. doi:10.1172/JCI66764.

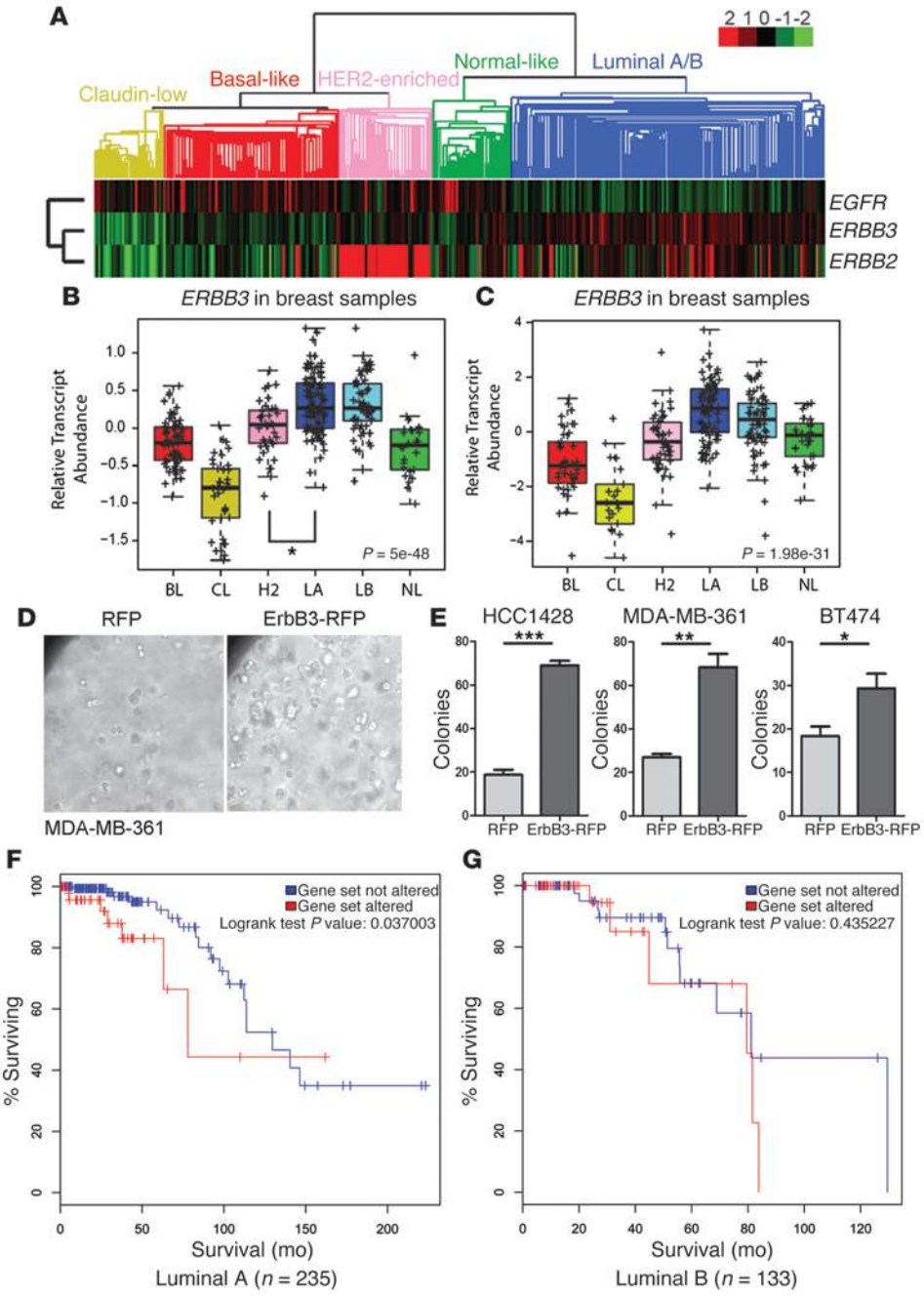

Figure 1
ErbB3 expression in luminal breast cancers. (**A**) cDNA microarray analysis of clinical breast cancers (UNC337 data set). Heat map shows expression of *EGFR*, *ERBB2*, and *ERBB3*. Each colored square represents relative transcript abundance (in $\log_2$ space) for each sample: lowest expression is green, highest is red, and average expression is black. The colored array tree denotes the intrinsic subtype of each sample. Dark blue, luminal A/B; green, normal-like; red, basal-like; pink, HER2-enriched; yellow, claudin-low). (**B** and **C**) *ERBB3* relative transcript levels across intrinsic molecular subtypes in the UNC337 data set (**B**) and an independently derived microarray data subset (**C**) (20, 21). BL, basal-like; CL, claudin-low; H2, HER2-enriched; LA, luminal A; LB, luminal B; NL, normal-like; Str, stromal. $^*P < 0.01$ (Student's *t* test). Midline shows the average ± SD. *P* values compare expression means across all groups. Midline shows the average. Whiskers show SD. Expression values in each tumor are shown by plus signs. *P* values compare expression means across all groups. (**D** and **E**) Luminal breast cancer cells were transduced with retrovirus expressing ErbB3-IRES-RFP. Puromycin-resistant cells overexpressing ErbB3 (1×10^3/well) were suspended in Matrigel (100 μl), cultured 10–14 days, photodocumented (**D**), and quantitated (**E**) using ImageJ software (NIH). Original magnification, ×100. Values shown represent the average number of colonies/well ± SD. $n = 3$. $^*P > 0.05$; $^{**}P > 0.01$; $^{***}P > 0.001$. (**F** and **G**) *ERBB3* gene copy number and mRNA expression levels were determined in TCGA-curated luminal A and luminal B breast cancers (23) and used to organize samples into those exhibiting *ERBB3* copy number gain or high ErbB3 expression (shown in red). Overall survival analysis was performed using cBio Portal (22).

that *ERBB3* mRNA expression was highest in luminal A/B tumors as compared with other clinical breast cancer molecular subtypes. In cell culture and xenograft models, targeting ErbB3 using the monoclonal antibody U3-1287 (17) impaired tumor cell growth and survival and improved tumor response to the ER inhibitor fulvestrant. Specifically, U3-1287 impaired fulvestrant-mediated compensatory signaling through the PI3K/Akt/mTOR pathway. These findings suggest that ErbB3 may have therapeutic value in luminal breast cancers.

Results

ERBB3 mRNA expression is highest in luminal breast cancers. Previous expression analyses revealed that *ERBB3* levels in the human breast epithelium are highest in luminal populations as compared with other epithelial cell types of the breast (12). To examine *ERBB3* expression across breast cancer molecular subtypes, we used a publicly available microarray data set (UNC337) derived from 320 human breast cancers and 17 normal breast specimens (18). Supervised hierarchical clustering of UNC337 using the intrinsic list (19) classified breast cancers into 5 molecularly defined subtypes: luminal A/B, *HER2*-enriched, basal-like, claudin-low and normal breast–like (Figure 1A). As expected, *HER2*-enriched breast cancers bore the highest levels of *ERBB2* expression, but relatively low *EGFR* and *ERBB3* levels. *EGFR* expression was highest among tumors of the basal-like, normal-like, and claudin-low subtypes, which expressed the lowest levels of *ERBB3*. Interestingly, *ERBB3* mRNA expression was highest among luminal A and luminal B tumors (which are

Table 1
ERBB3 copy number in breast cancer subtypes

	Luminial A	Luminal B	HER2-enriched	Basal-like	Claudin-low
ERBB3 copy number gain/amplification	29/235 (12.3%)	28/133 (21.1%)	16/58 (27.6%)	2/81 (2.5%)	0/8 (0%)
ERBB3 copy number loss (heterozygous and homozygous deletion)	7/235 (3%)	2/133 (1.5%)	2/58 (3.4%)	27/81 (33.3%)	2/8 (25%)

ERBB3 gene copy numbers were assessed by comparative genomic hybridization in 825 TCGA-curated breast cancers (23) and are shown based on PAM50-based molecular subtype classifications. Analysis was performed using cBio Portal (22).

largely ER positive) and lowest in basal-like and claudin-low subtypes (which are largely ER negative). The average level of *ERBB3* mRNA expression was determined for each molecularly defined breast tumor subtype, revealing a significant increase in *ERBB3* mRNA in luminal A and luminal B tumors over *HER2*-enriched, basal-like, claudin-low, and normal-like breast tumors (Figure 1B). These observations were verified in independent gene expression microarray data of 298 breast tumors (Figure 1C and refs. 20, 21). Analysis of clinical breast cancer specimens curated by The Cancer Genome Atlas (TCGA) (22, 23) revealed genomic *ERBB3* copy number gains in 12.3% and 21.1% of luminal A and luminal B tumors, respectively, and in 27.6% of *HER2*-enriched breast tumors. However, *ERBB3* copy number gains were seen in only 2.5% of basal-like tumors and were not detected in claudin-low tumors (Table 1). In contrast, *ERBB3* copy number losses were detected in 33.3% and 25% of basal-like and claudin-low breast tumors, respectively, but in only 3%, 1.5%, and 3.4% of luminal A, luminal B, and *HER2*-enriched breast tumors, respectively. *ERBB3* mRNA expression was elevated in luminal A/B tumors exhibiting *ERBB3* gene copy number gains as compared with those tumors with diploid *ERBB3* (Supplemental Figure 1; supplemental material available online with this article; doi:10.1172/JCI66764DS1). Taken together, these data demonstrate that in primary breast cancers, *ERBB3* mRNA expression correlates positively with the luminal A and luminal B subtypes, but not basal-like and claudin-low.

Luminal breast cancer cells utilize ErbB3 signaling for cell growth and survival. Because ErbB3 was expressed at high levels in luminal breast cancers, we examined the role of ErbB3 in luminal breast cancer cell lines. First, we overexpressed ErbB3 in ERα-positive luminal breast cell lines (Supplemental Figure 2), and cultured cells in 3D extracellular matrix (Matrigel) over 10 days (Figure 1D). ErbB3 overexpression increased colony growth in HCC1428 ($PIK3CA^{WT}PTEN^{WT}HER2^{WT}$), MDA-MB-361 ($PIK3CA^{E545K}PTEN^{WT}HER2^{WT}$), and BT474 ($PIK3CA^{K111N}PTEN^{WT}HER2^{AMP}$) cells (Figure 1E), suggesting that ErbB3 may enhance growth or progression of luminal breast tumors. This is consistent with TCGA-curated data demonstrating that luminal A breast tumors expressing high ErbB3 or with ErbB3 gene copy number gains exhibited decreased overall survival as compared with all other luminal A tumors (Figure 1F; $P = 0.037$). A correlation between *ErbB3* mRNA/gene copy number and patient survival was not observed in luminal B breast cancers from the TCGA data set (Figure 1G; $P = 0.435$).

Next, we tested the response of 3 luminal breast cancer–derived cell lines to U3-1287, a fully human monoclonal antibody directed against the human ErbB3 ectodomain. U3-1287 blocks ligand binding of ErbB3 and causes receptor downregulation (Figure 2A and ref. 24). Although growth of monolayer cultures of luminal breast cancer cell lines was not affected by U3-1287 (Supplemental Figure 3), single-cell suspensions of MCF7 ($PIK3CA^{E545K}PTEN^{WT}HER2^{WT}$), MDA-MB-361, and T47D ($PIK3CA^{H1047R}PTEN^{WT}HER2^{WT}$) cells embedded in Matrigel were growth inhibited over 14 days when cultured in the presence of U3-1287 (Figure 2B), resulting in decreased number of colonies in each cell line (Figure 2C). Based on these results, we assessed the effects of ErbB3 targeting of luminal breast tumors in vivo. MCF7, T47D, and MBA-MB-361 cells were injected into the inguinal mammary fat pads of BALB/c *nu/nu* female mice 24 hours after implantation of slow-release estrogen pellets. Tumors were palpable at 7–14 days and were subsequently measured twice weekly. Once tumors reached 100 mm^3, tumor-bearing mice were randomized into treatment groups receiving either U3-1287 (10 mg/kg, twice weekly) or control human IgG for 4 weeks. Histological analysis revealed that, while IgG-treated tumors comprised solid sheets of densely packed tumor cells, U3-1287–treated MCF7 tumors harbored large acellular areas (Figure 2D). Similar results were seen in T47D and MDA-MB-361 tumors (Supplemental Figure 4). U3-1287 significantly slowed the growth rate of MCF7 tumors, resulting in a 2-fold decrease in tumor volume as compared with IgG-treated tumors after 4 weeks of treatment (Figure 2E). Western analysis of whole-tumor lysates harvested after 7 days of treatment demonstrated that ErbB3 was downregulated in MCF7 tumors treated with U3-1287 as compared with those treated with IgG (Figure 2F). Similar results were seen in T47D tumor lysates (Supplemental Figure 5). Tumors treated with U3-1287 displayed modestly decreased phosphorylation of Akt (a target of PI3K signaling) in MCF7 and T47D lysates and robust inhibition of S6 (a target of mTOR signaling) in MCF7 lysates. This observation is consistent with the known role of ErbB3 in activating the PI3K/mTOR pathway in numerous ErbB receptor–dependent tumors (25–27), although MCF7, T47D, and other luminal breast cancer cells are not considered a model of EGFR or HER2 dependence.

Immunohistochemical analyses performed on tumors harvested after 7 days of treatment confirmed ErbB3 downregulation in U3-1287–treated MCF7 tumors (Figure 2G). Immunohistochemical detection of Ki67 was used to identify cycling cells within MCF7 xenografts, revealing decreased tumor cell proliferation in U3-1287–treated tumors (Figure 2G). The number of apoptotic cells, identified in situ using TUNEL, was increased in U3-1287–treated tumors as compared with IgG-treated controls (Figure 2G), suggesting that decreased cell growth and increased cell death contributed to the decreased tumor growth rate upon ErbB3 targeting with U3-1287. Although previous studies demonstrated that loss of ErbB3 during normal mammary gland development shifted the mammary epithelial population toward a more basal-like or mammary stem cell–like phenotype, we failed to see elevated expression of molecular markers of mammary stem cells or epithelial-mesenchymal transition in MCF7 cells treated with U3-1287 for 24 hours (Supplemental Figure 6).

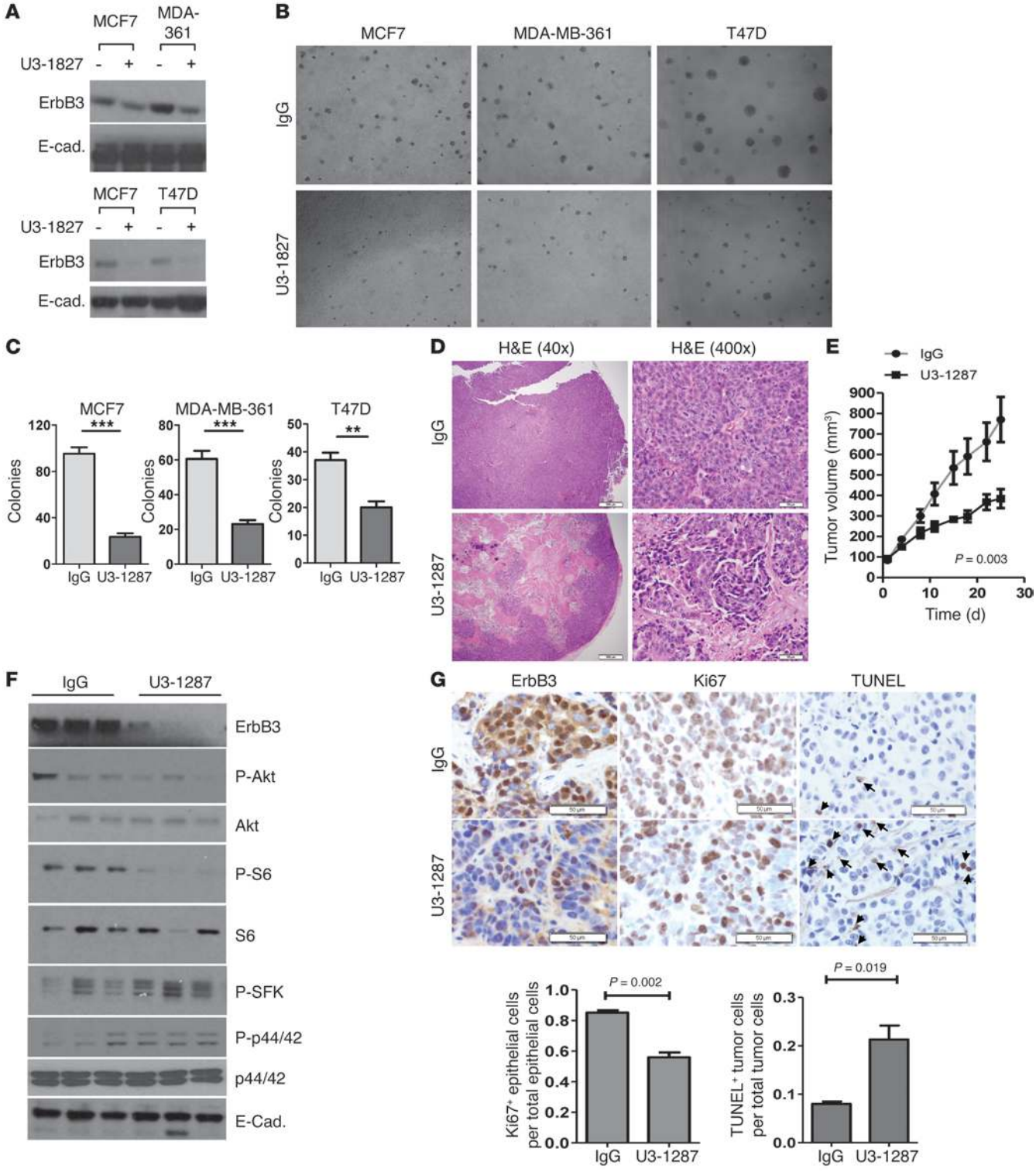
A
MCF7
MDA-361
U3-1827 - + - +
ErbB3
E-cad.
MCF7
T47D
U3-1827 - + - +
ErbB3
E-cad.
B
MCF7
MDA-MB-361
T47D
IgG
U3-1827
C
MCF7
MDA-MB-361
T47D
***
***
**
Colonies
IgG U3-1287
D
H&E (40x)
H&E (400x)
IgG
U3-1287
E
IgG
U3-1287
Tumor volume (mm3)
P = 0.003
Time (d)
F
IgG
U3-1287
ErbB3
P-Akt
Akt
P-S6
S6
P-SFK
P-p44/42
p44/42
E-Cad.
G
ErbB3
Ki67
TUNEL
IgG
U3-1287
P = 0.002
Ki67+ epithelial cells per total epithelial cells
IgG U3-1287
P = 0.019
TUNEL+ tumor cells per total tumor cells
IgG U3-1287

Figure 2
Pharmacological downregulation of ErbB3 decreases growth of luminal breast cancer cells. (**A**) Cells were cultured in medium with 10% serum plus U3-1287 (5 μg/ml) or isotype-matched human IgG for 24 hours, then used for Western blot analysis of whole-cell lysates using antibodies against ErbB3 and E-cadherin. (**B** and **C**) Cells were cultured in Matrigel for 14 days with the anti-ErbB3 antibody U3-1287 or isotype-matched human IgG. Colonies were imaged by photomicroscopy (**B**) and quantitated (**C**) using ImageJ software (NIH). Original magnification, ×100 (**B**). Representative images are shown in **B**. Values shown (**C**) are average ± SD, $n = 3$ per treatment group. $^{**}P < 0.01$; $^{***}P < 0.001$. (**D**–**F**) MCF7 tumor-bearing mice were randomized to receive normal human IgG or U3-1287 (5 mg/kg twice weekly). (**D**) Histological analysis of tumors on treatment day 28. Scale bars: 50 μm; Original magnification, ×400. (**E**) Average tumor volume ± SD for each treatment group is shown, $n = 10$. *P* value calculated using Student's *t* test to compare tumor volumes at day 28. (**F**) Whole-tumor lysates were assessed by Western analysis. Antibodies are shown at right. (**G**) Immunohistochemical detection of ErbB3-, Ki67-, and TUNEL-positive cells (arrows) is shown in tumor samples collected after 8 days of treatment. Representative images are shown. Scale bars: 50 μm. Values shown are the average ± SD of [(number of Ki67$^+$ or TUNEL$^+$) ÷ (number of epithelial tumor cells]. $n = 5$ samples, 4 fields per sample, Student's unpaired *t* test.

Fulvestrant-mediated upregulation of ErbB3 occurs at multiple levels. Previous studies demonstrated that ErbB3 expression is upregulated following fulvestrant treatment of MCF7 cells (28). We confirmed these findings in fulvestrant-treated MCF7 cells using immunofluorescent detection of ErbB3 (Figure 3A). Fulvestrant increased the number of cells expressing high levels of ErbB3, as measured by flow cytometry of fulvestrant-treated MCF7, ZR75-1, T47D, and BT474 cells (Figure 3B). While the number of MDA-MB-361 cells exhibiting high ErbB3 levels was unaltered in the presence of fulvestrant, perhaps due to the already high percentage of cells expressing ErbB3 in this cell line, the average intensity of ErbB3 staining per cell was elevated in fulvestrant-treated MDA-MB-361 cells as well as in MCF7, T47D, ZR75-1, and BT474.

Fulvestrant-induced ERα degradation correlated with upregulation of total ErbB3 protein expression in several luminal breast cancer cell lines, including cells with WT *PIK3CA* (HCC-1428), mutant *PIK3CA* (MCF7), and *PTEN* loss of function (ZR75-1, CAMA-1) (Figure 3C). Tyrosine phosphorylation of ErbB3 (Y1284) was induced in MCF7 cells within 24 hours of fulvestrant treatment (Figure 3D). Similarly, fulvestrant-treated *PIK3CA*-mutant cell lines T47D and MDA-MB-361 cells displayed ErbB3 upregulation within 16 hours of fulvestrant treatment (Figure 3E). To verify the upregulated species as ErbB3, we used siRNA-mediated knock-down of ErbB3, demonstrating impaired upregulation of ErbB3 protein expression in fulvestrant-treated MCF7 and T47D cells (Figure 3F). These results were confirmed by quantitative RT-PCR (qRT-PCR) to detect *ERBB3* in MCF7 cells treated with fulvestrant over a time course of 0–24 hours, demonstrating a 3-fold upregulation of *ERBB3* mRNA within 13 hours of fulvestrant treatment (Figure 3G). These finding were confirmed in a publicly available microarray data set (GSE14986) comparing mRNA expression profiles in DMSO-treated versus fulvestrant-treated MCF7 cells, revealing a 2.4-fold upregulation of *ERBB3* after 24 hours (Figure 3H). Transcripts encoding the ErbB3 ligand neuregulin-4 (NRG-4) and the ErbB3 heterodimeric partners ErbB2 and ErbB4 were also elevated 1.5-fold to 2.3-fold in response to fulvestrant, although transcript levels of *EGFR* and *NRG-1*, *-2*, and *-3* were not statistically altered by fulvestrant in this data set. Interestingly, *PA2G4*, the gene encoding ErbB3 binding protein (EBP) was downregulated in response to fulvestrant. EBP is a known negative regulator of ErbB3 signaling, although the mechanism by which this occurs is unclear. However, these expression changes predict that fulvestrant induces a transcriptional program that favors ErbB3 signaling. Consistent with these results, MCF7 cells transfected with a luciferase reporter driven by the proximal 1000 nucleotides upstream of the human ErbB3 transcriptional start site, pGL-ErbB3 (24), revealed a dose-dependent increase in ErbB3 transcription after 24 hours in the presence of fulvestrant (Figure 3I).

Actinomycin D treatment was used to inhibit de novo transcription, allowing us to measure how fulvestrant may affect *ERBB3* mRNA stability. Although 50% of *ERBB3* transcripts decayed within 8 hours of actinomycin D treatment in DMSO-treated cells (Figure 3J), *ERBB3* mRNA was not reduced in fulvestrant-treated cells after 8 hours of actinomycin D, consistent with increased stability of *ERBB3* transcripts in response to fulvestrant. Stability of ErbB3 protein was also enhanced in fulvestrant-treated cells, as demonstrated by measuring ErbB3 protein levels after treatment with an inhibitor of new protein synthesis, cycloheximide (Figure 3K). Thus, upregulation of ErbB3 expression in response to fulvestrant occurs at multiple levels of regulation, including transcriptional (Figure 3I), posttranscriptional (Figure 3J), and posttranslational (Figure 3K), although the precise mechanism by which ErbB3 is upregulated will require further investigation.

The impact of increased ErbB3 expression on tumor cell response to fulvestrant was examined in luminal breast cancer cell lines transduced with lentiviral ErbB3-IRES-RFP, or with RFP lentivirus. Single-cell suspensions were cultured 14 days in Matrigel in the presence of DMSO or fulvestrant (1 μM) (Figure 4). Fulvestrant decreased colony growth in all RFP-expressing cell lines tested. However, the cells expressing ErbB3 were resistant to growth inhibitory effects of fulvestrant.

Fulvestrant-mediated upregulation of ErbB3 is counteracted by U3-1287. To determine the impact of ErbB3 targeting in fulvestrant-treated cells, we first confirmed ErbB3 downregulation by U3-1287 in the presence and absence of fulvestrant. ErbB3 expression was downregulated in MCF7 and MDA-MB-361 cells treated with U3-1287, both in the presence and absence of fulvestrant (Supplemental Figure 7). Interestingly, downregulation of ErbB3 with U3-1287 resulted in decreased Tyr1056 phosphorylation of ErbB4, an NRG receptor and heterodimeric partner of ErbB3, without affecting total ErbB4 levels under basal conditions or upon fulvestrant-induced upregulation of ErbB4 (Supplemental Figure 8). These findings are significant, as previous studies demonstrate that ErbB3 and ErbB4 upregulation in response to fulvestrant drives NRG-mediated therapeutic resistance to fulvestrant (28). We confirmed that NRG/heregulin β1 (2 ng/ml) increased MCF7 monolayer growth in the presence of fulvestrant (Supplemental Figure 9). Although U3-1287 alone did not affect monolayer growth of MCF7, MDA-MB-361, and T47D cells, the combination of fulvestrant with U3-1287 decreased cell growth to a greater extent than fulvestrant alone (Supplemental Figure 10). Further, U3-1287 blocked NRG-mediated resistance to fulvestrant, suggesting that NRG requires ErbB3 to promote resistance to fulvestrant.

We further assessed the impact of U3-1287 on luminal breast tumor cell response to fulvestrant using single-cell suspensions cultured in 3D Matrigel. Single-agent U3-1287 reduced colony

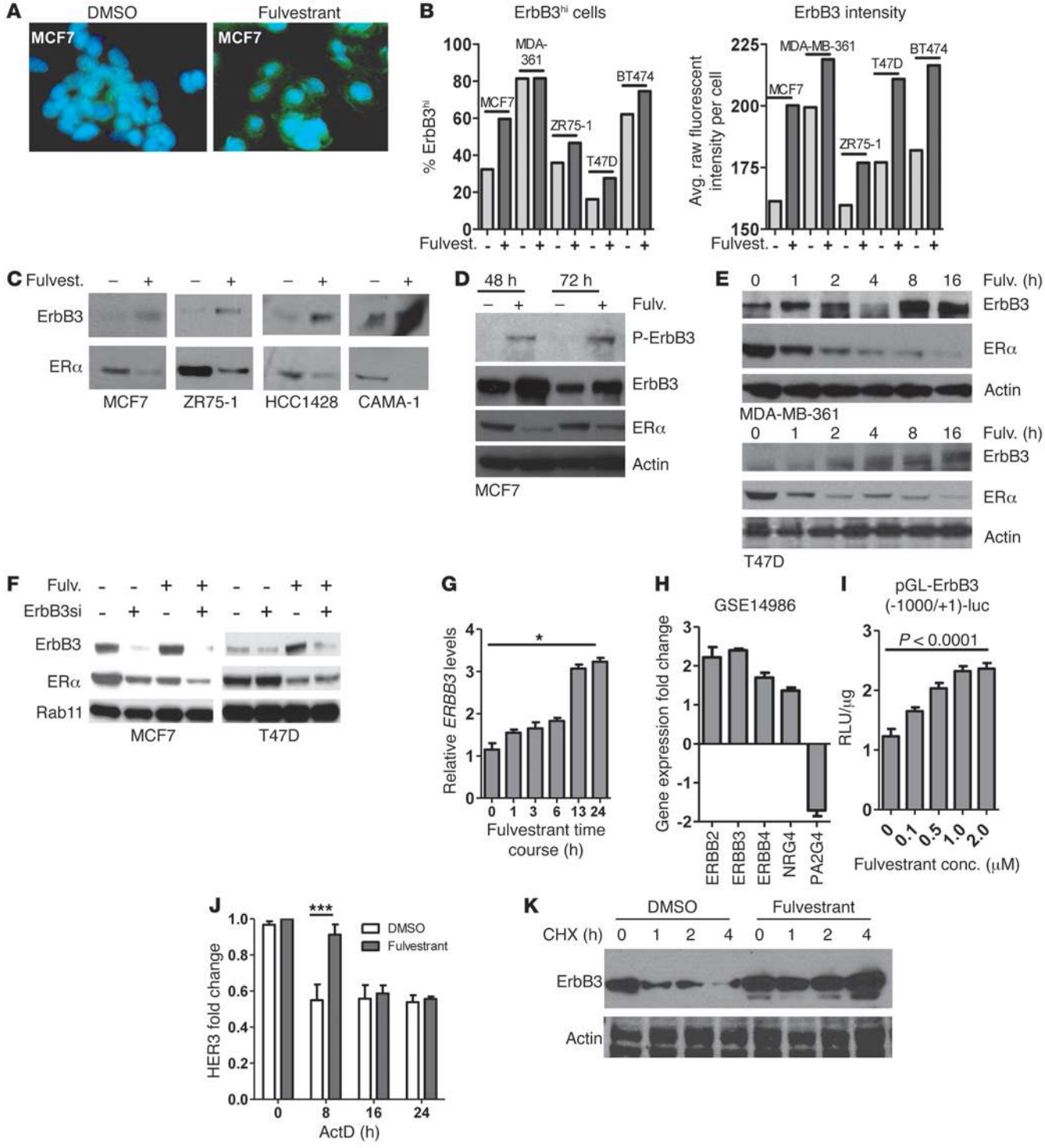
A
DMSO
Fulvestrant
MCF7
MCF7
B
ErbB3hi cells
% ErbB3hi
MDA-361
MCF7
ZR75-1
T47D
BT474
Fulvest.
ErbB3 intensity
Avg. raw fluorescent intensity per cell
MDA-MB-361
C
Fulvest.
ErbB3
ERα
MCF7
ZR75-1
HCC1428
CAMA-1
D
48 h
72 h
Fulv.
P-ErbB3
ErbB3
ERα
Actin
MCF7
E
Fulv. (h)
MDA-MB-361
T47D
F
Fulv.
ErbB3si
ErbB3
ERα
Rab11
MCF7
T47D
G
Relative ERBB3 levels
Fulvestrant time course (h)
H
GSE14986
Gene expression fold change
ERBB2
ERBB3
ERBB4
NRG4
PA2G4
I
pGL-ErbB3 (-1000/+1)-luc
P < 0.0001
RLU/μg
Fulvestrant conc. (μM)
J
DMSO
Fulvestrant
HER3 fold change
ActD (h)
K
DMSO
Fulvestrant
CHX (h)
ErbB3
Actin

Figure 3
Upregulation of ErbB3 signaling upon ER inhibition in luminal breast cancer cells. (**A** and **B**) Immunofluorescence (**A**) and flow cytometry (**B**) of ErbB3 in cells cultured for 24 hours with or without fulvestrant. Original magnification, ×200. (**B**) Left panel shows the ErbB3^{hi} percentage of cells (n = 50,000). Right panel shows average fluorescent intensity per cell. (**C**–**E**) Western blot analysis of cell lysates harvested after 0–72 hours of 1 μM fulvestrant. (**F**) Cells transfected with ErbB3-siRNA or control-siRNA were treated 24 hours with fulvestrant or DMSO prior to Western blot analysis for ErbB3 and ERα. (**G**) Real-time qPCR analysis of *ERBB3* in cells treated 0–24 hours with fulvestrant (1 μM). Average relative *ErbB3* levels shown ± SD. *P < 0.05, 1-way ANOVA. (**H**) Increased mRNA encoding ErbB receptors and ligands ± SD in fulvestrant-treated MCF7 cells measured in publicly available expression data (GSE14986). (**I**) MCF7 cells transfected with a human *ERBB3* gene promoter (–1000/+1) luciferase reporter plasmid were treated with increasing fulvestrant doses for 24 hours. Average (n = 3) RLUs per μg protein ± SD are shown. One-way ANOVA. (**J**) Real-time qPCR analysis of *ERBB3* mRNA in MCF7 cells treated 24 hours ± fulvestrant and actinomycin D (ActD). Average fold change is shown ± SD. ***P < 0.001. (**K**) Western blot analysis of fulvestrant-treated MCF7 lysates. Cycloheximide (CHX) was added for the final 0–4 hours.

growth (Supplemental Figure 11) and decreased total colony area in 3 of 6 cell lines tested (Figure 5A). While fulvestrant decreased colony growth in each of the 6 cell lines, the addition of U3-1287 resulted in a greater inhibition in total colony area as compared with what was seen with fulvestrant alone (Figure 5A), suggesting that fulvestrant-induced ErbB3 upregulation and signaling limits the potential therapeutic response to fulvestrant.

ErbB3 targeting using U3-1287 increases the response of luminal breast cancer cells to fulvestrant in vivo. MCF7 and MDA-MB-361 xenografts established in female nude mice supplanted with slow-release estrogen pellets were treated weekly with fulvestrant, with and without twice weekly U3-1287 treatment (10 mg/kg). Tumor volume was measured twice weekly during 42 days (MCF7) and 21 days (MDA-MB-361) of treatment. While MCF7 tumor growth was slowed by treatment with U3-1287 on its own and was also slowed by treatment with fulvestrant alone, the combination of fulvestrant with U3-1287 decreased tumor growth to a greater extent than that seen in tumors treated with either agent alone (Figure 5B). MCF7 tumor weight was 2.1-fold higher after 42 days of fulvestrant as compared with what was seen after 42 days of fulvestrant plus U3-1287 (Supplemental Figure 12). Similarly, MDA-MB-361 tumor growth was slowed by fulvestrant alone. However, the combination of fulvestrant plus U3-1287 decreased MDA-MB-361 tumor growth (Figure 5B) to a greater extent that fulvestrant alone and produced a 7-fold reduction in total tumor weight after 21 days of treatment (Supplemental Figure 13).

Histological examination of MCF7 tumors harvested at treatment day 42 revealed solid sheets of densely packed tumor cells in IgG-treated tumors (Figure 5C). The combination of fulvestrant with U3-1287 resulted in tumors comprising abundant extracellular matrix and sparse tumor cellularity. Similar histological effects were seen in T47D and MDA-MB-361 xenografts treated 14 days with the combination of U3-1287 and fulvestrant (Supplemental Figure 14).

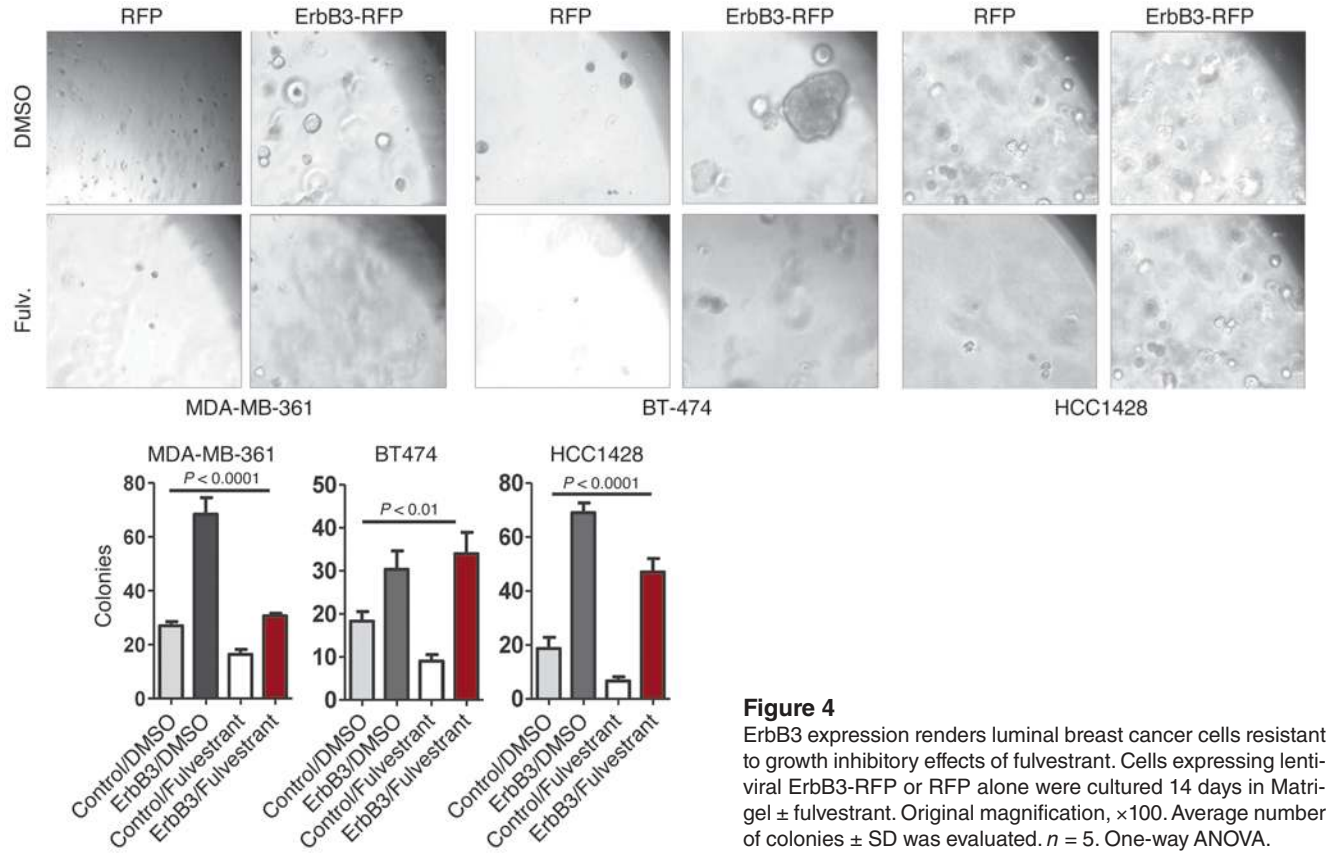

Figure 4
ErbB3 expression renders luminal breast cancer cells resistant to growth inhibitory effects of fulvestrant. Cells expressing lentiviral ErbB3-RFP or RFP alone were cultured 14 days in Matrigel ± fulvestrant. Original magnification, ×100. Average number of colonies ± SD was evaluated. n = 5. One-way ANOVA.

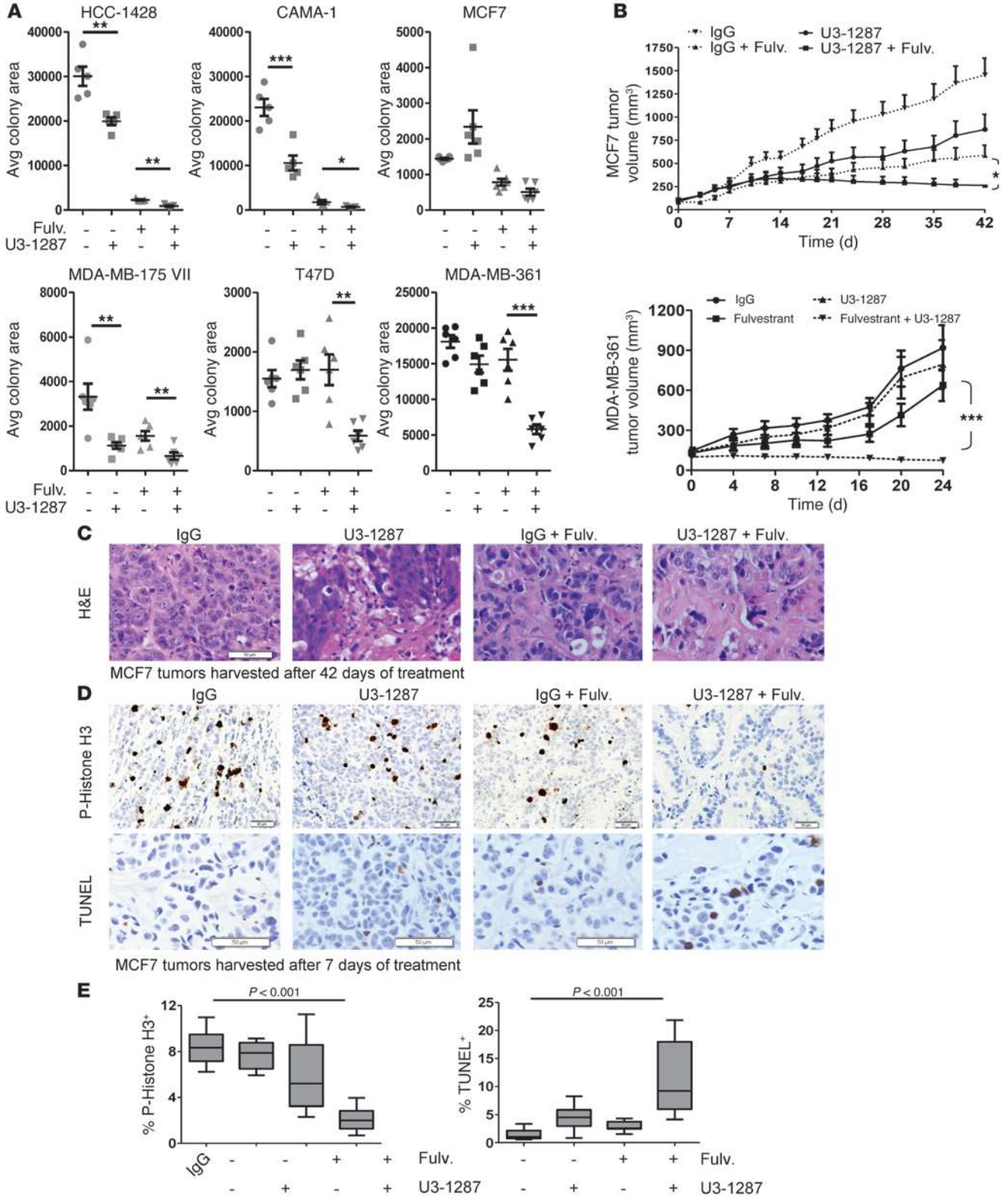
A
HCC-1428
CAMA-1
MCF7
MDA-MB-175 VII
T47D
MDA-MB-361
Avg colony area
Fulv.
U3-1287
B
IgG
IgG + Fulv.
U3-1287
U3-1287 + Fulv.
MCF7 tumor volume (mm3)
Time (d)
IgG
Fulvestrant
U3-1287
Fulvestrant + U3-1287
MDA-MB-361 tumor volume (mm3)
Time (d)
C
IgG
U3-1287
IgG + Fulv.
U3-1287 + Fulv.
H&E
MCF7 tumors harvested after 42 days of treatment
D
P-Histone H3
TUNEL
MCF7 tumors harvested after 7 days of treatment
E
P < 0.001
% P-Histone H3+
% TUNEL+
Fulv.
U3-1287

Figure 5
Luminal tumor response to the combination of U3-1287 and fulvestrant. (**A**) Luminal breast cancer cells (5×10^3) were embedded in Matrigel and cultured 14 days in the presence of U3-1287 (5 μg/ml) or control IgG with fulvestrant (1 μM) or DMSO. Photodocumented colonies were used to quantitate total colony area in ImageJ. Values represent the average colony area per field ± SD. $^{**}P < 0.01$; $^{***}P < 0.001$. (**B**–**E**) MCF7 and MDA-MB-361 xenograft–bearing mice were randomized into treatment arms to receive U3-1287 or IgG (each at 10 mg/kg, twice weekly) in the presence or absence of fulvestrant (once weekly). For MCF7 tumors: $n = 8$ (IgG); $n = 6$ (fulvestrant + IgG); $n = 10$ (U3-1287); $n = 10$ (U3-1287 + fulvestrant). For MDA-MB-361 tumors, $n = 10$ per group. Average tumor volumes ± SD are shown. (**B**) Tumor volume was measured throughout the treatment period. $^{*}P < 0.05$, comparing final tumor volumes, 2-way ANOVA. $^{***}P < 0.001$, comparing AUC, Student's *t* test. (**C**) Histological analysis of MCF7 tumors after 42 days of treatment. Scale bars: 50 μm. (**D**) Immunohistochemical detection of phospho-histone $H3^+$ and $TUNEL^+$ cells in MCF7 tumors after 8 days of treatment. Scale bars: 50 μm. (**E**) The average percentage ± SD of phospho-histone $H3^+$ or $TUNEL^+$ MCF7 tumor cells was determined. $n = 3$–4 per condition, 4 random fields per sample. *P* values calculated with 1-way ANOVA.

We used phospho-histone H3 immunohistochemistry (IHC) to detect mitotic cells. The proportion of phospho-histone $H3^+$ MCF7 tumor cells was reduced upon treatment with fulvestrant alone for 7 days (Figure 5, D and E). Although U3-1287 did not reduce phospho-histone $H3^+$ cells in MCF7 tumors, the combination of U3-1287 with fulvestrant produced a profound reduction in phospho-histone $H3^+$ cells (Figure 5E). While MCF7 tumors treated with either fulvestrant or U3-1287 displayed an increase in $TUNEL^+$ cells as compared with IgG-treated controls, the combination of fulvestrant with U3-1287 significantly increased the proportion of tumor cells that were $TUNEL^+$ over what was seen with either agent alone ($P < 0.01$ for either U3-1287 or fulvestrant compared with fulvestrant plus U3-1287). These results demonstrate that the combinatorial targeting of ER and ErbB3 produces superior inhibition of tumor growth through decreased tumor cell proliferation and survival.

Fulvestrant-mediated ErbB3 upregulation increases PI3K/mTOR signaling. Abundant evidence demonstrates that increased mTOR signaling drives resistance to endocrine inhibitors, an observation that underlies the clinical success of mTOR inhibitors (RAD001/everolimus) in combination with endocrine therapies (29). However, the mechanisms responsible for mTOR signaling in response to fulvestrant remain unclear. Because mTOR is a critical effector of the PI3K pathway and because ErbB3 is a potent activator of PI3K signaling, we tested the hypothesis that ErbB3-mediated PI3K activation drives mTOR signaling in response to fulvestrant. Using phosphorylation of ribosomal protein S6 (P-S6) as a surrogate marker of mTOR complex 1 (mTORC1) signaling, we found that fulvestrant-mediated ERα degradation coincided with P-S6 upregulation in MCF7, CAMA-1, T47D, and HCC1428 (Figure 6A) and MDA-MB-361 cells (Figure 6B). Fulvestrant-induced phospho-S6 was not seen in cultures treated with the mTORC1 inhibitor RAD001 for the final 2 hours of culture, confirming that fulvestrant induces S6 phosphorylation through increased mTORC1 signaling. This is consistent with the clinical observations that RAD001 improves clinical response to endocrine therapies (aromatase inhibitors) used to treat luminal breast cancers in the neoadjuvant setting (29). Heightened S6 phosphorylation was also seen in MCF7 xenografts after 7 days of fulvestrant treatment (Supplemental Figure 15).

mTORC1 is a downstream target of the PI3K/Akt pathway, but can be engaged by alternative signaling pathways as well. Therefore, to determine whether fulvestrant-induced ErbB3 signaling promotes mTOR activity through the PI3K pathway, we used small molecular weight kinase inhibitors to block precise steps in the PI3K/mTOR signal transduction cascade for the final 2 hours of culture. The Akt inhibitor MK2206 (1 μM) and the PI3K inhibitor BKM120 (0.5 μM) blocked fulvestrant-induced P-S6, suggesting that mTOR is activated downstream of PI3K/Akt in fulvestrant-treated cells (Figure 6A). The MEK inhibitor U0126 did not affect P-S6 upregulation in response to fulvestrant. Inhibition of PDK, a PI3K-activated kinase that phosphorylates Akt at T308, impaired fulvestrant-induced P-S6 (Supplemental Figure 16), while inhibition of serum glucose kinase (SGK), another PI3K-activated kinase, appeared to increase S6 phosphorylation under basal conditions and did not affect P-S6 levels in fulvestrant-treated cells. These data suggest that fulvestrant-treated cells upregulate mTORC1 through the PI3K-PDK-Akt signaling axis. Because ErbB3 is a potent activator of PI3K signaling, we examined the impact of ErbB3 inhibition with U3-1287 on fulvestrant-mediated mTOR activation in MCF7 cells. After 24 hours, fulvestrant increased phosphorylation of ErbB3 and P-S6 (Figure 6C), but U3-1287 blocked S6 phosphorylation in fulvestrant-treated cells. These data suggest that ErbB3 signaling drives mTOR activation in fulvestrant-treated cells through the PI3K pathway.

To determine whether fulvestrant in combination with ErbB3 inhibitors might result in growth inhibition comparable to that seen with fulvestrant in combination with the mTOR inhibitor RAD001, we assessed tumor cell death in cultures treated with fulvestrant for 24 hours in the presence of either U3-1287 or RAD001 (Supplemental Figure 17). Annexin V staining was used to enumerate dying cells, revealing that fulvestrant alone failed to increase tumor cell death in MCF7, MDA-MB-361, and T47D cells (Figure 6D). U3-1287 as a single agent significantly increased the number of annexin V–positive MCF7 and MDA-MB-361 cells ($P < 0.001$ in each cell line), but not T47D cells, but RAD001 failed to produce a statistically significant increase in cell death when used as a single agent in any cell line tested. In combination with fulvestrant, both U3-1287 and RAD001 increased cell death to a greater extent than either agent alone. However, the level of cell death was greater in response to U3-1287 plus fulvestrant as compared with RAD001 plus fulvestrant.

Previous studies have shown that signaling through mTORC1 produces negative feedback to the PI3K pathway. This would predict that mTORC1 inhibition might relieve this negative feedback, resulting in increased PI3K/Akt signaling, an event associated with therapeutic resistance. This idea was confirmed in MCF7 and MDA-MB-361 cells cultured with fulvestrant in the presence of RAD001, which demonstrated robust Akt phosphorylation at T308 (Supplemental Figure 18). However, the combination of U3-1287 with fulvestrant reduced Akt phosphorylation at T308 in both cell lines. These results suggest that ErbB3 targeting in combination with fulvestrant may restrain signaling through both the PI3K and the mTOR pathways, as opposed to mTOR inhibitors, which may allow signaling through the PI3K pathway. Because ErbB3 is known to activate PI3K signaling in response to ErbB family RTKS and also in response to heterologous RTKs (e.g., MET, FGFR2, IGF1R), we performed phospho-RTK array analysis

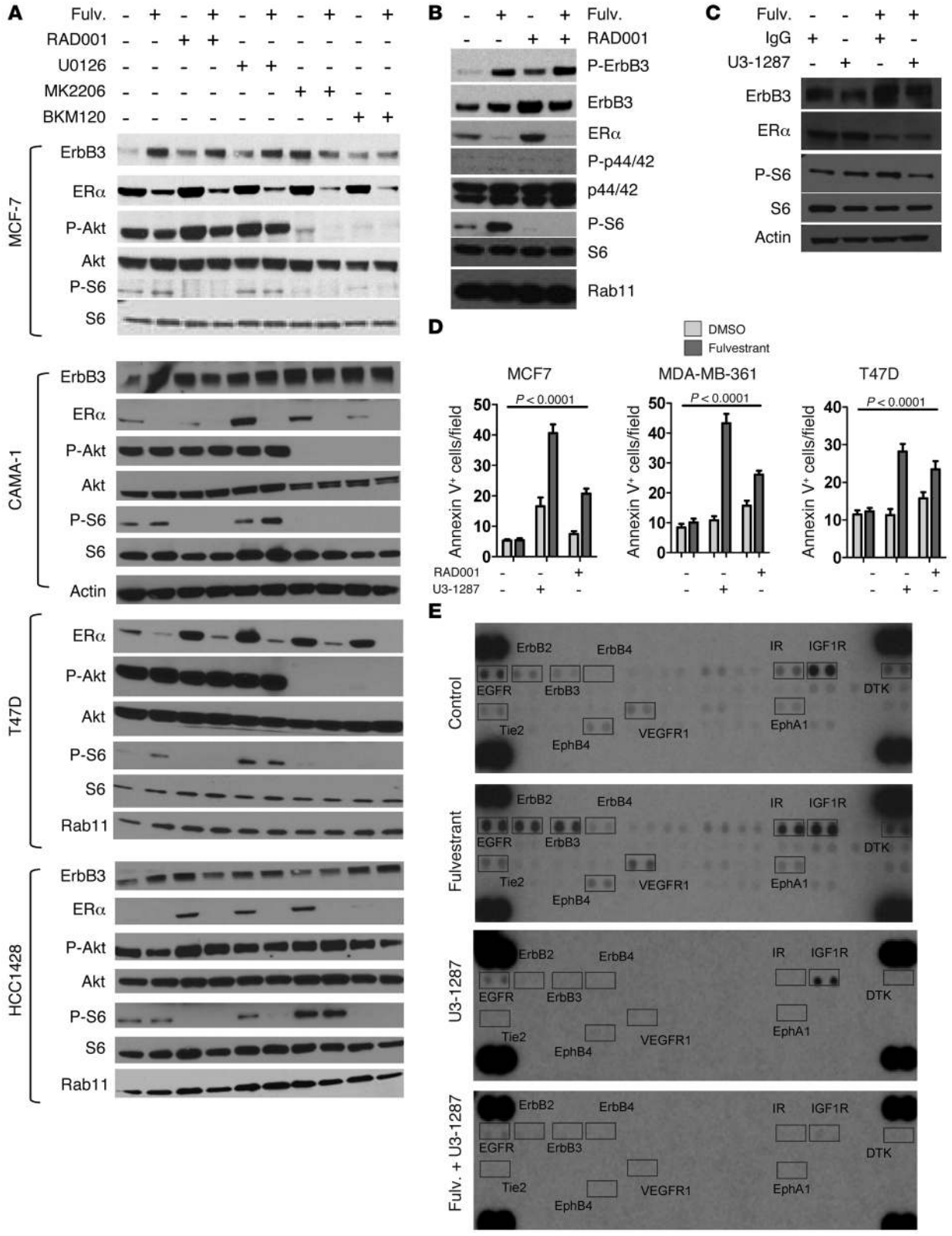
A
Fulv.
RAD001
U0126
MK2206
BKM120
MCF-7
CAMA-1
T47D
HCC1428
ErbB3
ERα
P-Akt
Akt
P-S6
S6
Actin
Rab11
B
Fulv.
RAD001
P-ErbB3
ErbB3
ERα
P-p44/42
p44/42
P-S6
S6
Rab11
C
Fulv.
IgG
U3-1287
ErbB3
ERα
P-S6
S6
Actin
D
DMSO
Fulvestrant
MCF7
MDA-MB-361
T47D
P < 0.0001
Annexin V+ cells/field
RAD001
U3-1287
E
Control
Fulvestrant
U3-1287
Fulv. + U3-1287
ErbB2
ErbB4
IR
IGF1R
EGFR
ErbB3
DTK
Tie2
EphB4
VEGFR1
EphA1

Figure 6
Fulvestrant-mediated mTOR upregulation requires signaling through the ErbB3-PI3K-Akt axis. (**A**) Western blot analysis of MCF7, CAMA-1, T47D, and HCC1428, whole-cell lysates harvested from serum-deprived cells after treatment for 48 hours with fulvestrant (1 μM), with the final 2 hours in the added presence of the mTOR inhibitor RAD001 (10 nM), the Akt inhibitor MK2206 (1 μM), the PI3K/p110α inhibitor BKM120 (0.5 μM), or the MEK inhibitor U0126 (5 μM). Antibodies used are indicated at the left of each panel. (**B**) Western blot analysis of MCF7 cells treated for 48 hours with fulvestrant or DMSO, and with RAD001 or DMSO for the final 2 hours of culture. Antibodies used are indicated. (**C**) Western blot analysis of MCF7 cells treated with fulvestrant (1 μM) or U3-1287 (5 μg/ml) for 48 hours prior to collection of whole-cell lysates. Antibodies used are indicated. (**D**) MCF7, T47D, and MDA-MB-361 cells were cultured 24 hours in the presence of fulvestrant (1 μM) or DMSO, U3-1287 (5 μg/ml) or control IgG, and RAD001 (0.2 μM) or DMSO. FITC-conjugated annexin V was added to the cultured medium to detect apoptotic cells. The number of FITC-labeled cells per ×600 field was measured using Scion Image 2.0 software. Values shown represent the average ± SD, $n = 3$. *P* values calculated with 1-way ANOVA. (**E**) RTK array was used to assess tyrosine phosphorylation of multiple RTKs in whole MCF7 tumor lysates.

of MCF7 whole-cell lysates cultured 24 hours in the presence of fulvestrant (Figure 6E). In addition to increased phospho-ErbB3, we found increased tyrosine phosphorylation of several RTKs in fulvestrant-treated cells as compared with what was seen in DMSO-treated cells, including insulin receptor (IR), IGF-1 receptor (IGF1R), and the ErbB family RTKs EGFR and ErbB2. However, ErbB3 targeting with U3-1287 reduced fulvestrant-induced ErbB3 tyrosine phosphorylation and also interfered with phosphorylation of EGFR, ErbB2, IGF1R, and IR. Notably, ErbB3 can heterodimerize with each of the ErbB family RTKs and has been detected in association with IGF1R. These results suggest that ErbB3 may be a keystone in fulvestrant-induced compensatory RTK responses. Consistent with this idea, expression analyses performed on RNA harvested from MCF7 xenografts treated 42 days with fulvestrant in the presence or absence of U3-1287 revealed substantial downregulation of breast cancer cell-cycle progression genes (*MKI67*, *TOP2A*, *CCNA2*, *SCGB1D2*, *TNFAIP2*) in tumors treated with the combination of U3-1287 and fulvestrant, but not in response to either agent when used alone (Supplemental Figure 19).

ErbB3 targeting decreases fulvestrant-induced PI3K/mTOR signaling in luminal breast cancer xenografts in vivo. These data suggest that ErbB3 may be central to feedback signaling that promotes resistance to endocrine therapy, particularly through the PI3K/mTOR pathway. Therefore, we measured ErbB3 and P-S6 levels in fulvestrant-treated MCF7, MDA-MB-361, and T47D xenografts. Although ErbB3 and P-S6 were detected in untreated MCF7 tumors by immunohistochemical analysis, profound upregulation of ErbB3 and P-S6 was seen after 7 days of fulvestrant treatment (Figure 7A), consistent with results obtained in clinical samples and in cell culture. U3-1287 did not appear to affect expression or nuclear localization of ERα and did not affect basal P-S6 levels in MCF7 xenografts. However, fulvestrant-induced upregulation of ErbB3 and P-S6 was largely impaired in the presence of U3-1287, as was phosphorylation of Akt at S473 in MCF7 xenografts (Figure 7B). Decreased phosphorylation of P-S6 and P-Akt was seen in T47D tumor lysates (Figure 7C) and MDA-MB-361 tumor lysates (Figure 7D).

We found similar results in paraffin sections of human breast tumor biopsies collected as part of a single-stage, single institution phase II neoadjuvant trial, in which postmenopausal women with newly diagnosed ER-positive breast cancer were treated for 4 months with anastrozole (Arimidex, an aromatase inhibitor) and fulvestrant (Faslodex) (30, 31). After a baseline tumor core biopsy on day 0, patients received anastrozole (1 mg daily), and fulvestrant (250 mg monthly). Pretreatment P-S6 and ErbB3 histo-score measurements were compared with P-S6 and ErbB3 histo-scores in matched samples from each patient collected after 21 days of treatment (Figure 7A). Increased tumor staining for ErbB3 was detected following endocrine therapy ($n = 4$), consistent with our results in cell culture models. We also detected increased P-S6 in ER^+ breast tumors following treatment with fulvestrant plus anastrozole (Figure 8A). Although the inclusion of the aromatase inhibitor anastrozole is a caveat of the clinical data set that is inconsistent with the fulvestrant-specific preclinical modeling described herein, these results support the idea that increased ErbB3 expression following antiestrogen therapy may be biologically meaningful. Feedback regulation through signaling pathways that utilize ErbB3 may be a mechanism by which luminal breast cancers drive PI3K/mTOR signaling to reduce sensitivity to hormonal therapy. Importantly, reverse phase protein analysis of whole-tumor lysates harvested from 235 luminal A breast tumors (TCGA-curated breast tumors) revealed that those tumors exhibiting *ERBB3* gene copy number gain displayed increased P-S6 and increased phosphorylation of p70-S6 kinase as compared with those harboring diploid *ERBB3* (Figure 8B and ref. 22). These results support a model in which ErbB3 signaling through PI3K/mTOR drives cell growth and survival, even in the face of therapeutic ERα inhibition (Figure 8C).

Discussion

Advances in molecular analysis of primary tumors make it clear that different subtypes of human breast cancer exist (32). Intense research efforts are focused on understanding the molecular characteristics defining each group and how those characteristics influence prognosis and/or should affect advice regarding treatment decisions within a given breast cancer subtype. EGFR overexpression is often found in basal-like breast cancers (33). ErbB2/HER2 overexpression due to *HER2* gene amplification results in formation of *HER2*-related breast cancers (27). There is little consensus about the role of ErbB4 in models of breast cancer, perhaps due to the multitude of splice variations affecting its signaling capabilities and biological outcomes or due to its role in promoting secretory differentiation of the breast epithelium (34). Because ErbB3 is kinase impaired, its role in breast cancer has been framed by its ability to heterodimerize with HER2 and EGFR (26, 35). ErbB3 tyrosine phosphorylation is often seen in ErbB2-overexpressing breast cancers (36, 37). The ErbB2/ErbB3 heterodimer forms a powerful oncogenic unit, based in part on the ability of ErbB3 to amplify signaling through PI3K (4, 26, 38, 39). However, we found that *ERBB3* mRNA levels were highest in luminal A/B breast cancers, a molecular subtype in which ErbB3 signaling is relatively understudied. These results are consistent with recent findings that ErbB3 is required for cell survival in the untransformed luminal mammary epithelium, but not the untransformed basal epithelium (12). Because transformation of a luminal mammary epithelial cell (MEC) may give rise to a luminal breast cancer (15, 16), it is possible that the molecular pathways regulating luminal MEC development may be commandeered by luminal breast tumors to promote growth and survival. Understanding the confluence of these signaling pathways will yield a greater understanding of how

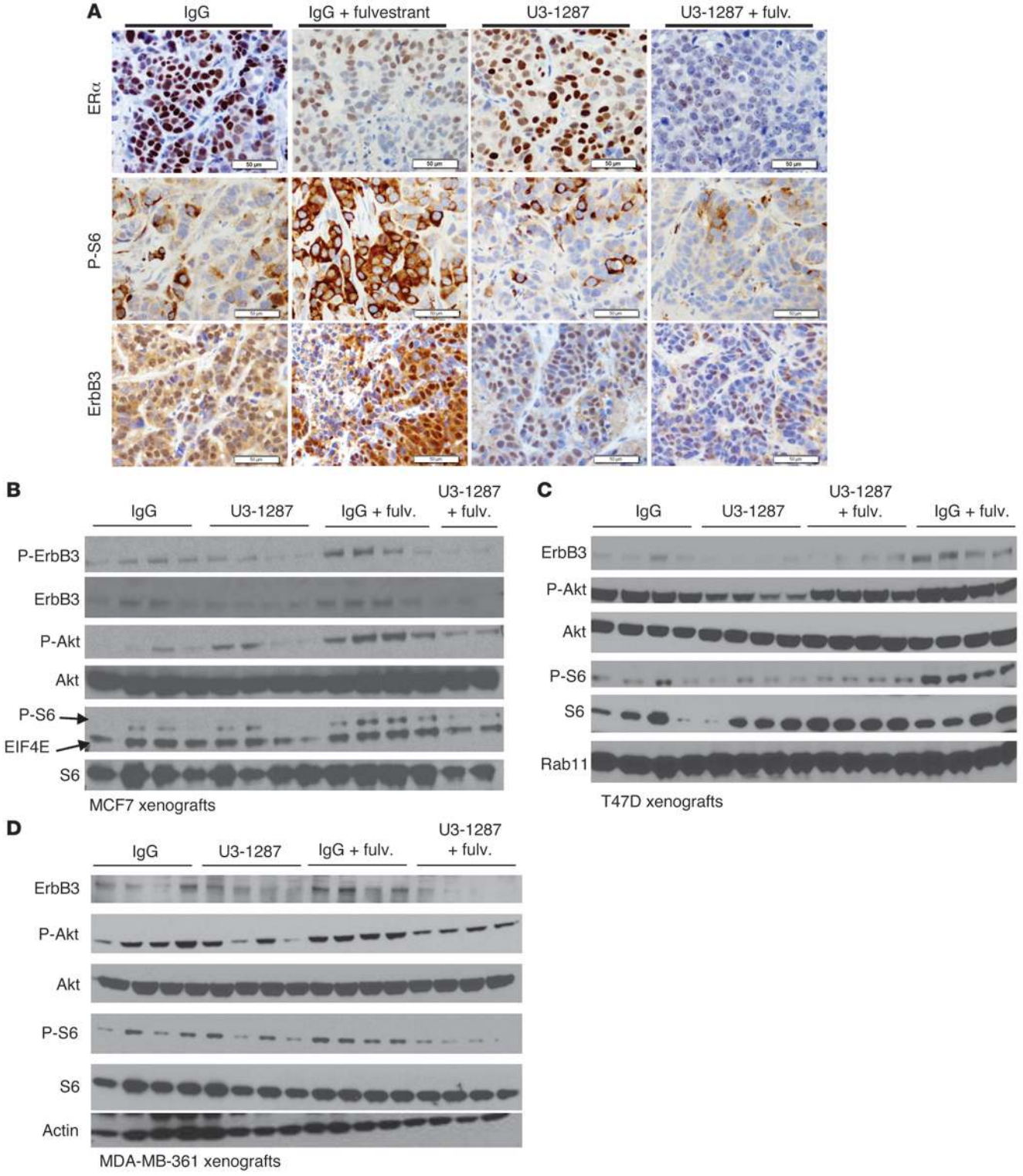

Figure 7

Feedback signaling through ErbB3 limits innate tumor response to endocrine therapy but can be targeted with U3-1287. (**A**) MCF7 xenografts treated with U3-1287 or IgG (each at 20 mg/kg, twice weekly) in the presence or absence of fulvestrant (once weekly) were collected at day 8 of treatment (24 hours after the second fulvestrant treatment). Immunohistochemical analysis was used to detect ErbB3, P-S6, and ERα. Scale bars: 50 μm. (**B**–**D**) Western blot analysis of tumor xenografts from mice treated with fulvestrant with and without U3-1287 for 8 days. Tumors were harvested 24 hours after the final treatment with U3-1287 and fulvestrant. Antibodies used are indicated.

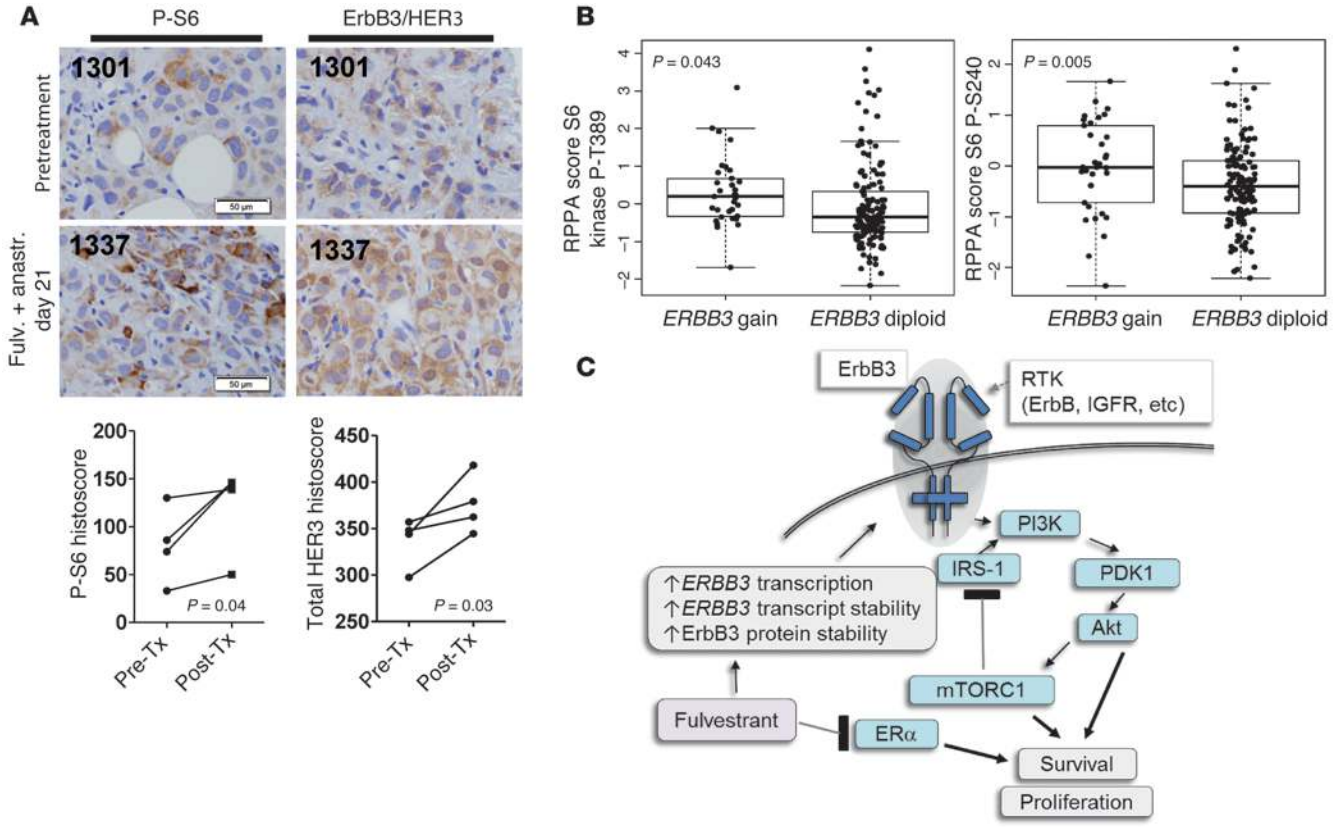

Figure 8

Fulvestrant-treated clinical breast tumors demonstrate ErbB3 and P-S6 upregulation. (**A**) Matched pairs of clinical breast cancer specimens collected 24 hours prior to treatment (day 0) and 21 days after a single treatment with fulvestrant on day 1 followed by daily treatment with anastrozole (day 21) were assessed by IHC. ErbB3 and P-S6 expression was assessed by IHC. Intensity of total ErbB3 immunostaining (cytoplasmic and membrane) and P-S6 immunostaining were quantified. Values shown represent the average ± SD (n = 4). P values trended toward significance (P = 0.06, Student's paired t test). A representative matched pair is shown. Scale bars: 50 μm. (**B**) TCGA-curated luminal A breast cancers were separated into those tumors exhibiting *ERBB3* copy number gain on those with diploid *ERBB3*, then assessed for differences in phospho-proteins as detected by RPPA analysis. P-S6 and P-S6 kinase were significantly increased in tumors exhibiting *ERBB3* copy number gain. (Student's t test). (**C**) Model of how luminal breast cancers use ErbB3-PI3K signaling to limit their intrinsic sensitivity to fulvestrant. ERα targeting with fulvestrant drives ErbB3 upregulation at the cell surface through transcriptional, posttranscriptional, and posttranslational mechanisms. Increased ErbB3 enhances PI3K signaling through its 6 PI3K interaction motifs. PI3K activates PDK1, which phosphorylates Akt. Once activated, Akt promotes mTORC1 activation, driving increased S6-kinase and S6 phosphorylation.

to prevent and treat breast cancers. We have shown that ErbB3 drives growth and survival of luminal breast cancers, which is similar to its role in the development of the luminal mammary epithelium. It is now presented as a potential therapeutic target to improve the response of luminal breast cancers to antihormonal therapy.

Previous reports demonstrate that ErbB3 is important in endocrine resistance in luminal breast cancer cells genetically engineered to overexpress *HER2* or to lack *PTEN*. However, we describe herein that ErbB3 upregulation is not a genetic event that is imposed, selected for, or acquired over time, but instead is a mechanism inherent to many luminal breast cancer cells and one that limits therapeutic response to fulvestrant. Therefore, our findings are not limited to those breast cancer cells harboring *HER2* gene amplification or *PTEN* deletion. We have included numerous luminal cell lines with physiological and pathological levels of HER2, EGFR, and PTEN and cell lines expressing WT *PIK3CA* or mutant *PIK3CA* (Supplemental Table 1). We have used large clinical breast cancer data sets to demonstrate that luminal breast cancers uniformly express *ERBB3* mRNA levels that exceed what is seen for transcripts encoding EGFR and HER2. Given that ErbB3 on its own has only weak tyrosine kinase activity, ErbB3 should not be categorized so readily as equivalent to HER2 and EGFR, which are highly active tyrosine kinases that phosphorylate downstream targets. Our results demonstrate that ErbB3, despite being kinase impaired, is a valid therapeutic target even in the absence of HER2 or EGFR overexpression. These observations will cause breast cancer scientists to reevaluate their preconceptions regarding how ErbB3 affects tumor cell signaling. Since ErbB3 relies on transphosphorylation by heterodimeric partners to drive signal transduction, the observation that *ERBB3* expression is highest in breast cancers expressing lower levels of EGFR and ErbB2 would suggest other tyrosine kinases may phosphorylate ErbB3 in luminal breast cells. We postulate 3 plausible scenarios that are not mutually exclusive and are likely to operate together. First, ErbB3/ErbB4 heterodimerization may drive ErbB3 tyrosine phosphorylation and signal transduction in luminal breast cancers. Notably, the highest levels of *ERBB4* mRNA are seen in luminal breast tumors over other molecular subtypes (40, 41). Secondly, ErbB3 may become tyrosine phosphorylated independently of ErbB heterodimeriza-

tion. This idea is supported by observations that ErbB3 can be transphosphorylated by heterologous RTKs, including Met and FGFR2 (42, 43). Previous findings suggest that ErbB3 activation is rapidly induced by IGF-1 signaling, consistent with the idea that IGF1R contributes to ErbB3 phosphorylation in luminal breast cancers (44, 45) and together may promote resistance to endocrine therapy (45, 46). A third possibility is that low levels of EGFR and/or ErbB2 are sufficient for phosphorylation of ErbB3 and that their upregulation in response to fulvestrant drives ErbB3 tyrosine phosphorylation and compensatory PI3K signaling.

In summary, higher levels of ErbB3 expression in luminal breast cancers (as compared with other breast cancer subtypes) drives growth and survival of several ER-positive breast cancer cell lines. Upregulation of ErbB3 in response to fulvestrant was seen in clinical breast specimens and was modeled in luminal breast cancer–derived cells, revealing that ErbB3 targeting improved the therapeutic effect of fulvestrant by limiting ErbB3-induced signaling through PI3K/mTOR. These findings demonstrate that ErbB3 targeting using an antibody-based approach may improve the outcome of patients treated with antiendocrine therapies.

Methods

Human breast tumor gene expression analysis. The publicly available microarray data sets queried for tumor gene expression data were the UNC337 (18) and the NKI295 (20, 21, 32, 47–49). PAM50 and claudin-low intrinsic subtype cells in UNC337 and NKI295 were used as published previously (18). The MAQC-II project: human breast cancer (BR) data set constituting 230 breast tumors was extracted from GEO (GSE20194) and utilized to compare *ERBB3* expression among molecular subtypes. TCGA (23) Invasive Breast Cancer data set was clustered according to PAM50 subtypes, and corresponding data on *ERBB3* mRNA and gene copy number, patient survival, and phospho-S6 protein levels were analyzed using publicly available software on the cBio Portal website (22).

Xenograft experiments. Estrogen pellets (14 days extended release, 0.17 mg β estradiol; Innovative Research of America) were implanted subcutaneously into 3- to 4-week-old female BALB/c athymic nude mice (Harlan Laboratories). Right and left inguinal mammary fat pads were injected with 10^6 MCF7, MDA-MB-361, or T47D cells in 100 μl growth factor–reduced Matrigel. Tumors were measured with calipers twice weekly. Tumor-bearing mice were randomized into treatment arms to receive U3-1287 (provided by U3 Pharma GmbH) or normal human IgG (5 mg/kg, each delivered twice weekly by intraperitoneal injection) in the presence or absence of fulvestrant (Novartis) delivered once weekly by intraperitoneal injection.

Histological analysis. Sections (5-μm) were stained with H&E. In situ TUNEL analysis was performed on paraffin-embedded sections using the ApopTag kit (Calbiochem). IHC on paraffin-embedded sections was performed using the following antibodies as described previously (13): ErbB3, phospho-histone H3, and Ki67 (Santa Cruz Biotechnology Inc.), P-S6 (Cell Signaling Technologies), and ERα (Neomarkers). Immunodetection was performed using the Vectastain kit (Vector Laboratories) according to the manufacturer's directions.

Western blotting. Cells were homogenized in ice-cold lysis buffer (50 mM Tris, pH 7.4, 100 mM NaF, 120 mM NaCl, 0.5% NP-40, 100 μM Na_3VO_4, 1X protease inhibitor cocktail; Roche). Proteins were used for Human Phospho-RTK array (R&D Systems) according to the manufacturer's directions or were separated on NuPage polyacrylamide gels (Life Technologies) and transferred to nitrocellulose membranes. Membranes were blocked and probed with antibody as previously described (12). The following primary antibodies were used: ErbB3 (C-17, 1:1000; Santa Cruz Biotechnology Inc.); Y1197 P-ErbB3 (1:1000; Cell Signaling Inc.); ErbB4 (1:1000; Santa Cruz Biotechnology Inc.); α-actin (1:5000; Sigma-Aldrich); MAPK, P-MAPK, S6, P-S6, AKT, and S473 P-Akt (1:1000; Cell Signaling Technologies).

Cell culture. All human breast cancer cell lines (MCF7, T47D, MDA-MB-361) were obtained from ATTC and were cultured in DMEM supplemented with 10% FBS (Atlanta Biologics) except where indicated as serum-free. Fulvestrant (Sigma-Aldrich), BKM120 (Novartis), MK-2206 (Selleck Chem), PDK1 inhibitor (Calbiochem), RAD001 (Sigma-Aldrich), and heregulin-1β epidermal growth factor-like domain (R&D Systems) were used where indicated. Colony assays were seeded in 6-well dishes (10^5 cells/dish) and cultured 14 days in DMEM/10% FBS. Cells were fixed in formalin, stained with crystal violet, and imaged on a flatbed scanner.

Immunofluorescence. Cells were fixed 10 minutes in 10% formalin, permeabilized in 100% methanol, blocked in 3% gelatin, stained with rabbit anti-ErbB3 (1:100; Santa Cruz Biotechnologies) and goat anti-rabbit Alexa Fluor 488 (1:100) and mounted with VectaStain+ DAPI (Vector Laboratories). Images were captured using the ProgRes MF digital camera (Jenoptiks) mounted on the Motic AE31 microscope. Images were minimally processed in Microsoft Publisher (for contrast only).

Flow cytometry. Cells were collected by gentle trypsinization, fixed and permeabilized (BD Cytofix/Cytoperm), and stained with phycoerythrin-conjugated mouse anti-human ErbB3 (1:50; R&D Systems). Data were acquired using the FACSCalibur flow cytometer and Cell Quest software. 50,000 events were assessed per sample by forward and side scatter gating performed on software (Cytobank.org).

Immunohistochemical analysis of ErbB3 in clinical breast tumor specimens. Paraffin sections of human breast tumor biopsies collected as part of a single stage, single institution a phase II neoadjuvant trial testing the combined effects of anastrozole (Arimidex), fulvestrant (Faslodex), and gefitinib (Iressa) in postmenopausal women with newly diagnosed ER-positive breast cancer (30, 31) were assessed by immunohistochemical staining with antibodies against ErbB3 as described previously (24). The pathologist reading the results was blinded to the treatment group (day 1 versus 21).

RNA extraction and quantitative RT PCR. See Supplemental Methods.

Statistics. To assess statistical significance in experiments directly comparing an experimental group with a control group, Student's unpaired, 2-tailed *t* test was used. To assess statistical significance in experiments in which multiple groups were compared across a single condition, 1-way ANOVA was used. To compare the response of 2 agents combined to either single agent alone, 2-way ANOVA was used. $P < 0.05$ was considered significantly different from the null hypothesis.

Study approval. All animal experimentation was performed in AAALAC-approved facilities at Vanderbilt University Medical Center. All animal use protocols were reviewed and approved prior to experimentation by the Institutional Animal Care and Use Committee at Vanderbilt University.

Acknowledgments

This work was supported by the NIH R01CA143126 (to R.S. Cook), R01CA80195 (to C.L. Arteaga), P50 CA98131, P50 CA058223, and P50 CA58183, and P30 CA68485, Susan G. Komen for the Cure grant KG100677 (to R.S. Cook), ACS Clinical Research Professorship grant CRP-07-234 (to C.L. Arteaga), the Lee Jeans Translational Breast Cancer Research Program (to C.L. Arteaga), and Stand Up To Cancer grant "Targeting PI3K in Women's Cancers" (to C.L. Arteaga).

Received for publication March 8, 2013, and accepted in revised form July 3, 2013.

Address correspondence to: Rebecca S. Cook, Vanderbilt University School of Medicine, Department of Cancer Biology, 2220 Pierce Avenue, Rm 749 Preston Research Building, Nashville, Tennessee 37232, USA. Phone: 615.936.3813; Fax: 615.936.2911; E-mail: rebecca.cook@vanderbilt.edu.

1. Abd El-Rehim DM, et al. Expression and co-expression of the members of the epidermal growth factor receptor (EGFR) family in invasive breast carcinoma. *Br J Cancer*. 2004;91(8):1532–1542.
2. Citri A, Yarden Y. EGF-ERBB signalling: towards the systems level. *Nat Rev Mol Cell Biol*. 2006; 7(7):505–516.
3. Bazley LA, Gullick WJ. The epidermal growth factor receptor family. *Endocr Relat Cancer*. 2005; 12(suppl 1):S17–S27.
4. Holbro T, Civenni G, Hynes NE. The ErbB receptors and their role in cancer progression. *Exp Cell Res*. 2003;284(1):99–110.
5. Carraway KL, et al. The erbB3 gene product is a receptor for heregulin. *J Biol Chem*. 1994; 269(19):14303–14306.
6. Pinkas-Kramarski R, et al. Diversification of Neu differentiation factor and epidermal growth factor signaling by combinatorial receptor interactions. *EMBO J*. 1996;15(10):2452–2467.
7. Kim HH, Vijapurkar U, Hellyer NJ, Bravo D, Koland JG. Signal transduction by epidermal growth factor and heregulin via the kinase-deficient ErbB3 protein. *Biochem J*. 1998;334(pt 1):189–195.
8. Franklin MC, Carey KD, Vajdos FF, Leahy DJ, de Vos AM, Sliwkowski MX. Insights into ErbB signaling from the structure of the ErbB2-pertuzumab complex. *Cancer Cell*. 2004;5(4):317–328.
9. Cook RS, et al. ErbB3 ablation impairs phosphatidylinositol 3-kinase (PI3K)/AKT-dependent mammary tumorigenesis. *Cancer Res*. 2011;71(11):3941–3951.
10. Vaught DB, et al. HER3 is required for HER2-induced pre-neoplastic changes to the breast epithelium and tumor formation. *Cancer Res*. 2012; 72(10):2672–2682.
11. Herschkowitz JI, et al. Identification of conserved gene expression features between murine mammary carcinoma models and human breast tumors. *Genome Biol*. 2007;8(5):R76.
12. Balko JM, et al. The receptor tyrosine kinase ErbB3 maintains the balance between luminal and basal breast epithelium. *Proc Natl Acad Sci U S A*. 2012; 109(1):221–226.
13. Qu S, et al. Gene targeting of ErbB3 using a Cre-mediated unidirectional DNA inversion strategy. *Genesis*. 2006;44(10):477–486.
14. Jackson-Fisher AJ, et al. ErbB3 is required for ductal morphogenesis in the mouse mammary gland. *Breast Cancer Res*. 2008;10(6):R96.
15. Lindeman GJ, Visvader JE. Insights into the cell of origin in breast cancer and breast cancer stem cells. *Asia Pac J Clin Oncol*. 2010;6(2):89–97.
16. Visvader JE. Cells of origin in cancer. *Nature*. 2011; 469(7330):314–322.
17. Arnett SO, Teillaud JL, Wurch T, Reichert JM, Dunlop C, Huber M. IBC's 21st Annual Antibody Engineering and 8th Annual Antibody Therapeutics International Conferences and 2010 Annual Meeting of the Antibody Society. December 5-9, 2010, San Diego, CA USA. *MAbs*. 2011;3(2):133–152.
18. Prat A, et al. Phenotypic and molecular characterization of the claudin-low intrinsic subtype of breast cancer. *Breast Cancer Res*. 2010;12(5):R68.
19. Parker JS, et al. Supervised risk predictor of breast cancer based on intrinsic subtypes. *J Clin Oncol*. 2009; 27(8):1160–1167.
20. van de Vijver MJ, et al. A gene-expression signature as a predictor of survival in breast cancer. *N Engl J Med*. 2002;347(25):1999–2009.
21. van 't Veer LJ, et al. Gene expression profiling predicts clinical outcome of breast cancer. *Nature*. 2002;415(6871):530–536.
22. Cerami E, et al. The cBio cancer genomics portal: an open platform for exploring multidimensional cancer genomics data. *Cancer Discov*. 2012;2(5):401–404.
23. Cancer Genome Atlas Network. Comprehensive molecular portraits of human breast tumours. *Nature*. 2012;490(7418):61–70.
24. Garrett JT, et al. Transcriptional and posttranslational up-regulation of HER3 (ErbB3) compensates for inhibition of the HER2 tyrosine kinase. *Proc Natl Acad Sci U S A*. 2011;108(12):5021–5026.
25. Hellyer NJ, Cheng K, Koland JG. ErbB3 (HER3) interaction with the p85 regulatory subunit of phosphoinositide 3-kinase. *Biochem J*. 1998; 333(pt 3):757–763.
26. Holbro T, Beerli RR, Maurer F, Koziczak M, Barbas CF, Hynes NE. The ErbB2/ErbB3 heterodimer functions as an oncogenic unit: ErbB2 requires ErbB3 to drive breast tumor cell proliferation. *Proc Natl Acad Sci U S A*. 2003;100(15):8933–8938.
27. Stern DF. ERBB3/HER3 and ERBB2/HER2 duet in mammary development and breast cancer. *J Mammary Gland Biol Neoplasia*. 2008;13(2):215–223.
28. Hutcheson IR, et al. Fulvestrant-induced expression of ErbB3 and ErbB4 receptors sensitizes oestrogen receptor-positive breast cancer cells to heregulin beta1. *Breast Cancer Res*. 2011;13(2):R29.
29. Baselga J, et al. Everolimus in postmenopausal hormone-receptor-positive advanced breast cancer. *N Engl J Med*. 2012;366(6):520–529.
30. Massarweh S, et al. A phase II neoadjuvant trial of anastrozole, fulvestrant, and gefitinib in patients with newly diagnosed estrogen receptor positive breast cancer. *Breast Cancer Res Treat*. 2011; 129(3):819–827.
31. Samarnthai N, Elledge R, Prihoda TJ, Huang J, Massarweh S, Yeh IT. Pathologic changes in breast cancer after anti-estrogen therapy. *Breast J*. 2012; 18(4):362–366.
32. Sorlie T, et al. Gene expression patterns of breast carcinomas distinguish tumor subclasses with clinical implications. *Proc Natl Acad Sci U S A*. 2001; 98(19):10869–10874.
33. Livasy CA, et al. Phenotypic evaluation of the basal-like subtype of invasive breast carcinoma. *Mod Pathol*. 2006;19(2):264–271.
34. Muraoka-Cook RS, Feng SM, Strunk KE, Earp HS. ErbB4/HER4: role in mammary gland development, differentiation and growth inhibition. *J Mammary Gland Biol Neoplasia*. 2008;13(2):235–246.
35. Alimandi M, et al. Cooperative signaling of ErbB3 and ErbB2 in neoplastic transformation and human mammary carcinomas. *Oncogene*. 1995; 10(9):1813–1821.
36. Tovey SM, Witton CJ, Bartlett JM, Stanton PD, Reeves JR, Cooke TG. Outcome and human epidermal growth factor receptor (HER) 1-4 status in invasive breast carcinomas with proliferation indices evaluated by bromodeoxyuridine labelling. *Breast Cancer Res*. 2004;6(3):R246–R251.
37. Witton CJ, Reeves JR, Going JJ, Cooke TG, Bartlett JM. Expression of the HER1-4 family of receptor tyrosine kinases in breast cancer. *J Pathol*. 2003; 200(3):290–297.
38. Siegel PM, Ryan ED, Cardiff RD, Muller WJ. Elevated expression of activated forms of Neu/ErbB-2 and ErbB-3 are involved in the induction of mammary tumors in transgenic mice: implications for human breast cancer. *EMBO J*. 1999;18(8):2149–2164.
39. Lee-Hoeflich ST, et al. A central role for HER3 in HER2-amplified breast cancer: implications for targeted therapy. *Cancer Res*. 2008;68(14):5878–5887.
40. Sundvall M, Iljin K, Kilpinen S, Sara H, Kallioniemi OP, Elenius K. Role of ErbB4 in breast cancer. *J Mammary Gland Biol Neoplasia*. 2008;13(2):259–268.
41. Hoadley KA, et al. EGFR associated expression profiles vary with breast tumor subtype. *BMC Genomics*. 2007;8:258.
42. Engelman JA, et al. MET amplification leads to gefitinib resistance in lung cancer by activating ERBB3 signaling. *Science*. 2007;316(5827):1039–1043.
43. Kunii K, et al. FGFR2-amplified gastric cancer cell lines require FGFR2 and Erbb3 signaling for growth and survival. *Cancer Res*. 2008;68(7):2340–2348.
44. Knowlden JM, et al. erbB3 recruitment of insulin receptor substrate 1 modulates insulin-like growth factor receptor signalling in oestrogen receptor-positive breast cancer cell lines. *Breast Cancer Res*. 2011; 13(5):R93.
45. Miller TW, et al. Loss of Phosphatase and Tensin homologue deleted on chromosome 10 engages ErbB3 and insulin-like growth factor-I receptor signaling to promote antiestrogen resistance in breast cancer. *Cancer Res*. 2009;69(10):4192–4201.
46. Fox EM, et al. A kinome-wide screen identifies the insulin/IGF-I receptor pathway as a mechanism of escape from hormone dependence in breast cancer. *Cancer Res*. 2011;71(21):6773–6784.
47. Sorlie T, et al. Repeated observation of breast tumor subtypes in independent gene expression data sets. *Proc Natl Acad Sci U S A*. 2003;100(14):8418–8423.
48. Chang HY, et al. Robustness, scalability, and integration of a wound-response gene expression signature in predicting breast cancer survival. *Proc Natl Acad Sci U S A*. 2005;102(10):3738–3743.
49. Miller LD, et al. An expression signature for p53 status in human breast cancer predicts mutation status, transcriptional effects, and patient survival. *Proc Natl Acad Sci U S A*. 2005;102(38):13550–13555.